2

Surface-Barrier Solar Cells Based On Monocrystalline Cadmium Telluride with the Modified Boundary

P.M. Gorley[1], V.P. Makhniy[1], P.P. Horley[1,2],
Yu.V. Vorobiev[3] and J. González-Hernández[2]
[1]*Science and Education Center "Semiconductor Material Science and Energy-Efficient Technology" at Yuri Fedkovych Chernivtsi National University, 58012 Chernivtsi,*
[2]*Centro de Investigación en Materiales Avanzados S.C., Chihuahua / Monterrey, 31109 Chihuahua,*
[3]*Centro de Investigación y de Estudios Avanzados del IPN, Unidad Querétaro, 76230 Querétaro,*
[1]*Ukraine*
[2,3]*México*

1. Introduction

Cadmium telluride is one of the most promising materials for solar cell (SC) applications due to its unique physical and chemical parameters. In the first place, it has the band gap $E_g \approx 1.5$ eV (300 K) close to the optimal value for photovoltaic conversion (Fahrenbruch & Bube, 1983; Donnet, 2001). The highest temperature and radiation stability of CdTe in comparison with Si and GaAs (Ryzhikov, 1989; Korbutyak et al., 2000) permits to use SCs based on cadmium telluride under elevated temperatures and a considerable flux of ionizing radiation. The possible alternative to CdTe with the similar band gap – gallium arsenide and its solid solutions – are far more difficult to obtain and expensive due to the rarity of Ga (Mizetskaya et al., 1986; Kesamanly & Nasledov, 1973; Andreev et al., 1975).

Solar cells may use diode structures of different kind: p-n-junction, heterojunction (HJ) or surface barrier contact. Despite CdTe has a bipolar conductivity, creation of p-n junction cell based on it is impractical due to high resistivity of p-CdTe and technological difficulty to make ohmic contacts to this material. Therefore, heterojunctions offer more versatile solution by allowing larger parameter variation of junction components than those acceptable for p-n junctions (Alferov, 1998). Additionally, direct band gap of cadmium telluride allows to use this material in thin film form, which was confirmed experimentally for thin film junction nCdS/pCdTe (Sites & Pan, 2007). Alas, the crystalline parameters and coefficients of thermal expansion for CdS (as well as the other semiconductors with wider band gap) significantly differ from those of CdTe (Milnes & Feucht, 1972; Sharma & Purohit, 1979; Simashkevich, 1980), so that the resulting HJ would inherit a significant concentration of the defects at the junction boundary, which will decrease the performance of the solar

Source: Solar Energy, Book edited by: Radu D. Rugescu,
ISBN 978-953-307-052-0, pp. 432, February 2010, INTECH, Croatia, downloaded from SCIYO.COM

cell. Moreover, despite the low cost of thin film cells comparing to those based on the bulk material, the technology for the thin-film CdTe has a significant perspectives to be improved (Chopra & Das, 1983; Britt & Ferekides, 1993). Therefore, it seems more appropriate to use monocrystalline cadmium telluride, which has well established and reliable technology (Ryzhikov, 1989; Korbutyak et al., 2000; Mizetskaya et al., 1986). It is preferable to design a technological method for manufacturing photovoltaic devices that could be easily adapted for creation of similar structures based on thin film form of CdTe after minute correction of the corresponding technological regimes.

For this type of applications, surface-barrier diode (SBD) is definitely a good candidate due to its advantages over other diode types (Strikha & Kil'chitskaya, 1992) – simple single-cycle technology necessary to create mono- and multi-element photodiodes of arbitrary area and topology over mono- or poly-crystalline substrates, as well as anomalously low temperatures of barrier contact deposition so that the parameters of the base substrates do not undergo any significant changes in the process. Additionally, substrates of any conductivity type are suitable for formation of SBDs, including those with pre-deposited ohmic contacts. The presence of a strong sub-surface electric field favors efficient separation of non-equilibrium carriers generated by the high-energy phonons. Finally, SBDs can have much lower values of series resistance R_0 comparing with the p-n junctions and hetero-junctions, as they have one semiconductor region in place of two.

However, many of the recent papers (Amanullah, 2003; Mason et al., 2004; Kim et al., 2009, 2009; Gnatyuk et al., 2005; Higa et al., 2007) are rather dedicated to ionizing radiation detectors based on high-resistive CdTe. In contrast with SC, here the surface effects are of far lower importance because ionizing particles penetrate deeper into the material. Independently on the application area of the SBD devices, they should have the largest possible height of the potential barrier. Analysis of literature sources points the impossibility to obtain SBDs with high barrier, minimal series resistance and surface recombination rate using the traditional technological methods (Milnes & Feucht, 1972; Strikha & Kil'chitskaya, 1992; Rhoderick, 1978; Valiev et al., 1981; Sze & Kwok, 2007) – thus, the new methodology should be involved.

One of the perspective ways to solve this problem involves technologies that modify the sub-surface properties of the base substrates, at the same time keeping parameters of bulk material free from significant changes. Here we analyze the experimental results concerning electrical, optical and photoelectric properties of n-CdTe substrates with the modified substrate and surface-barrier solar cells based on them.

2. Objects and methodology of investigations

The base substrates with dimensions 4×4×1 mm^3 were cut from the bulk CdTe monocrystal, grown by Bridgeman method. The base material featured intrinsic defect electron conductivity 0.1 – 0.05 $\Omega^{-1}\cdot cm^{-1}$ at 300 K as was not doped during the growth process. The substrates were polished mechanically and chemically in the solution of $K_2Cr_2O_7$:H_2O:HNO_3 in proportion 4:20:10 with further rinsing in de-ionized water. As a result, the surface of the substrates gained a mirror-reflective look, and the samples featured a weak photo-luminescence (PL) at 300 K. The similar luminescence is also observed for the cleft surfaces, but it is completely absent in the mechanically-polished plates.

One of the largest sides of the plates with the mirror-reflective surface was deposited with indium ohmic contacts by soldering. Before the creation of a rectifying contact, which was formed with a semitransparent layer of gold deposited by vacuum sputtering, the contact-

bearing side of the substrate was subjected to a different additional treatment. The first group of the samples was annealed in the air; further on, they will be referred to as CdTe:O_2 (Makhniy et al., 2009). The second group was processed in boiling aquatic suspension of base metal salts (Li_2CO_3, K_2CO_3 and Na_2CO_3), further addressed CdTe:AS (Makhniy & Skrypnyk, 2008). The third group of the samples was formed by chemically-etched substrates not subjected to any additional treatment; these will be further referred to as CdTe. The SBDs based on them served as reference material for comparative studies of modified surface diodes made of the samples belonging to CdTe:O_2 and CdTe:AS groups.

The dark current-voltage and capacitance-voltage curves (CVC and CpVC) were measured using the common methodology (Vorobiev et al., 1988; Batavin et al., 1985). The luminescence of the samples was excited with He-Ne and N_2-lasers (wave lengths 0.63 and 0.337 μm, respectively). The radiation, reflection and transmission spectra (N_ω, R_ω and T_ω) were obtained with a universal setup, allowing measurements in standard and differential modes (Makhniy et al., 2004). The spectra were registered automatically with a recording equipment KS-2, also allowing to obtain relaxation curves for the photoluminescence intensity. The light source for measurements of reflection and transmission spectra was a xenon lamp with a smooth spectrum in the investigated energy ranges. All the obtained spectra were corrected for non-linearity of the measuring system. PL spectra were plotted as a number of photons per unitary energy interval N_ω versus photon energy $\hbar\omega$.

The light source used for measuring of photoelectric characteristics was an incandescent lamp with a tungsten filament and a deuterium lamp. Fine tuning of the illumination level in the ranges of 4-5 orders of magnitude was done using a set of calibrated filters. The integral light and loading characteristics of the solar cell were measured with a common methodology (Koltun, 1985; Koltun, 1987). To study the spectral distribution of photosensitivity S_ω we used monochromator DMR-4 with energy dispersion 0.5 – 6.0 eV and precision 0.025 eV/mm. The Si and ZnSe photodiodes with known absolute current sensitivity were used as reference detectors.

The temperature measurements were performed in the ranges 300 – 450 K. The sample was deposited into a specially designed thermal chamber allowing appropriate illumination, quick variation and steady temperature maintenance with the precision of ±1 K. The photovoltaic efficiency of the solar cells was studied by comparing their photoelectric parameters with the reference ITO-Si cell, which under 300 K had the efficiency of 10% for AM2 illumination.

3. Optical properties

As it was shown by the previous studies (Makhniy et al., 2004), the surface modification of the n-CdTe substrates changes their optical properties in a different way depending on the annealing conditions. This approach also works for CdTe:AS and CdTe:O_2 samples featuring a sharp efficiency increase for the edge A-band of luminescence η (Fig. 1), which at 300 K can reach several percents. At the same time, for the substrates with mirror-reflecting surface this parameter does not exceed 0.01%. As the effective length of laser radiation in cadmium telluride is $\ell_{PL} \leq 10^{-5}$ cm, the photoluminescence takes place in a narrow sub-surface layer. Therefore, the luminescence intensity I_{PL} in the first approximation can be considered inversely proportional to the concentration of surface defects N_S. As surface modification decreases this concentration for more than two orders of magnitude, it makes a good motivation to use the substrates with modified surface for photodiode applications sensitive in short-wave region.

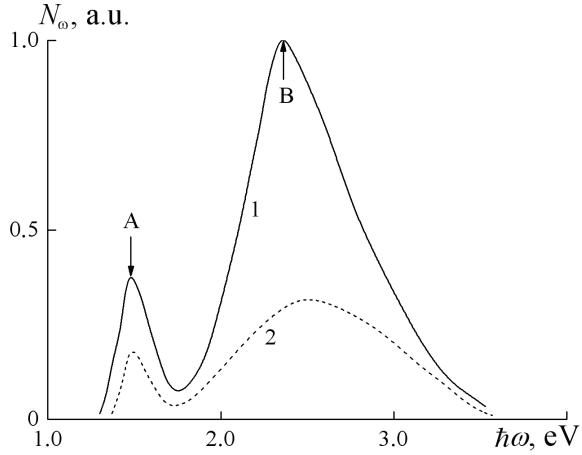

Fig. 1. PL spectra for the substrates CdTe:O_2 with 1) free surface and 2) covered with a golden film

To the contrast to CdTe:AS, the PL spectra of CdTe:O_2 samples feature a wide B-band situated in the intrinsic absorption area of CdTe at $\hbar\omega > E_g$, Fig. 1. The half-width $\Delta\hbar\omega_{1/2}$ of this band at 300 K is about 0.7 – 0.8 eV. It was found that the intensity of this high-energy band changes with time but that of A-band remains stable, also the peak of A-band $\hbar\omega_m$ shifts towards the low-energy region. It is important to mention that the stationary values of intensity I_{PL} and energy $\hbar\omega_m$ can be achieved several minutes after enabling the laser excitation (Fig. 2). Photoluminescence spectrum shown in Fig. 1, curve 1, was measured namely under such conditions. The experimental dependence of time constant for B-band $t_{1/2}(T)$ can be described by the Arrhenius law (inset to Fig. 2) with activation energy ~ 0.2 eV.

Our investigations revealed that the deposition of a semitransparent golden film onto the surface of CdTe:O_2 stabilizes I_{PL} (Fig. 2, curve 2). Despite the figure shows only the initial part of the $I_{PL}(t)$ curve, it remains unchanged not only after several hours, but also after switching laser illumination on and off for several times. This result is very important from the applied point of view, because semitransparent golden film works as an efficient barrier contact required for the optimal performance of SCs based on CdTe:O_2 substrates (Ciach et al., 1999).

The existence of high-energy B-band in the PL spectra of CdTe:O_2 samples can be explained by quantization of carrier energy caused by the presence of nano-scale structure formations, which is confirmed with the images obtained by the AFM Nanoscope-III in the periodic contact mode (Fig. 3). As one can see, the surface of annealed CdTe:O_2 samples is composed with granules some 10 – 50 nm in size (Fig. 3a), which may eventually join into a larger (100 – 500 nm) formations (Fig. 3b).

Annealing the samples under the optimal conditions (e.g., temperature and time) will result in optimization of A-band intensity corresponding to the edge luminescence (Makhniy et al., 2009). Using the relation $I_{PL} \sim N_S^{-1}$, one may come to the conclusion that such high-luminescent samples should have the minimal surface recombination rate. The AFM image of such substrates CdTe:O_2 reveals formation of nano-grains of various sizes (Fig. 3b). It is

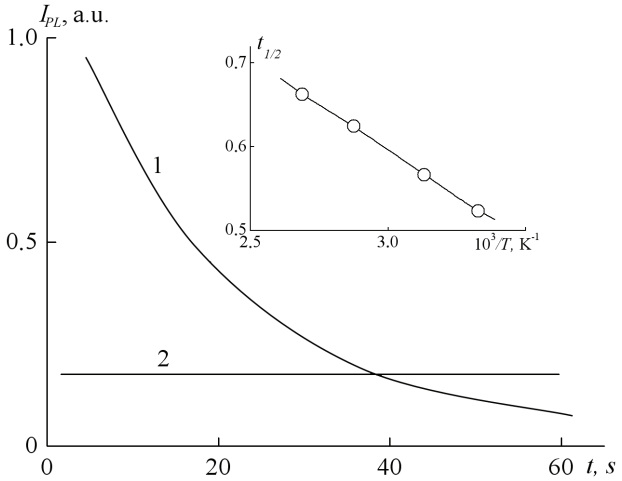

Fig. 2. Time dependence of B-band intensity at 300 K for CdTe:O_2 samples 1) with free surface and 2) covered with golden film. The inset shows the temperature dependence of time variable $t_{1/2}$

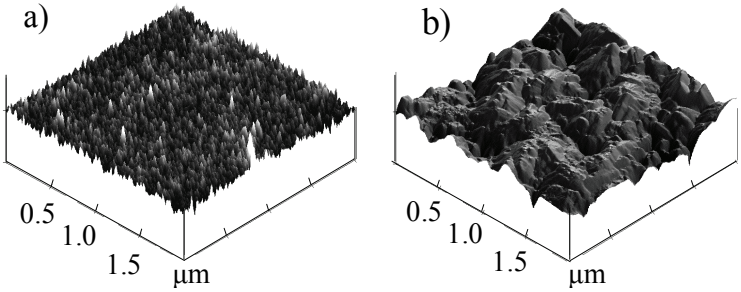

Fig. 3. AFM images of a) the original and b) air-annealed n-CdTe substrates

worth mentioning that large and small grains play a different role for the properties of surface-modified CdTe:O_2. The transition energy is defined by the quantization rule (Zayachuk, 2006; Pool & Owens, 2006)

$$\Delta E = \frac{n^2\hbar^2}{2d^2}\left(\frac{1}{m_n^*}+\frac{1}{m_p^*}\right), \tag{1}$$

where m_n^* and m_p^* are the effective masses of electron and a hole; d is lateral dimension of nano-object responsible for the energy peak $\hbar\omega_m$ in the PL spectrum. The depth of the quantum well for such objects is

$$\Delta E = \hbar\omega_m - E_g\ . \tag{2}$$

Using the values m_n^* = 0.11 m_0; m_p^* = 0.35m_0; E_g=1.5 eV and $\hbar\omega_m$≈2.5 eV defined from the experiment, we applied expressions (1) and (2) to estimate nano-particle dimension d to be

about 5 nm, which is two times smaller than the minimum observed size of the small grains ($d \approx 10$ nm) appearing in the AFM images. This controversy can be removed taking into account that the majority of the grains have a pyramidal shape (Fig. 3b), so that the B-band may be formed by contribution from their top parts, which are narrower than their base. The secondary proof of such possibility consists in presence of the photons with energy $\hbar\omega > \hbar\omega_m$, most probably caused by nano-objects with dimensions smaller than 5 nm.

It is important to emphasize that B-band can not be caused by the luminescence of CdO film that may be eventually formed during the annealing process. In the first place, we did not observe any visible radiation for the samples with CdO film created by photo-thermal oxidation over the substrates with mirror-smooth surface. Moreover, the differential reflection spectrum R_ω' of such samples has a peak corresponding to E_g of cadmium oxide, which is absent in the spectra of the modified substrates, Fig. 4.

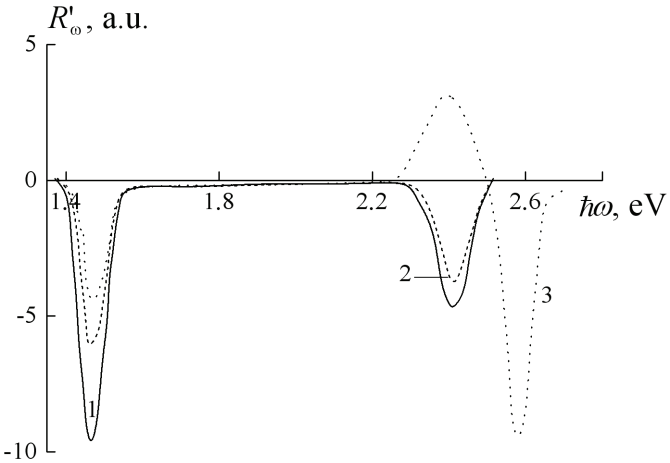

Fig. 4. Differential reflection spectra for various substrates: 1) CdTe, 2) CdTe:O_2 and 3) heterostructures CdO/CdTe at T = 300 K

The peaks located at 1.5 and 2.4 eV will correspond to the energy distance between the conduction band E_C and the edges of the valence band: the main sub-band E_{VA} and spin-orbital split band E_{VB}. The peak at $\hbar_{\omega m} \approx 2.6$ eV correlates with the band gap of CdO at 300 K (Madelung, 2004). The high-energy "tail" of B-band continues much further than it should if being solely defined by E_g(CdTe). It is worth noting that optical transmission / absorption of the samples is defined with the sample group. The "smooth" transmission curve T_ω for CdTe and CdTe:AS substrates has a sharp high-energy edge at $\hbar_{\omega m} \approx 1.5$ eV corresponding to the band gap of CdTe, Fig. 5.

In contrast, the samples annealed in the air feature a significant decrease of T_ω with red-shifted high-energy transmission edge intercepting the abscissa axis at the energy 1.3 eV, which is significantly lower than E_g of cadmium telluride. The detected peculiarities of transmission spectrum can be explained by the presence of super-grains (100 – 500 nm in size) at the surface of the samples. Such grains may cause light scattering and multiple reflections decreasing the absolute value of T_ω. As these processes intensify for the larger $\hbar\omega$, it may be the cause of the observed red-shift of T_ω curve. It is worth mentioning that in the

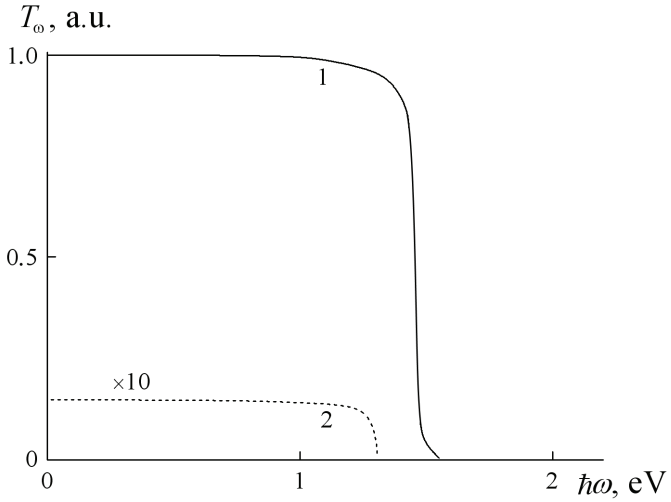

Fig. 5. Optical transmission spectra for different substrates: 1) CdTe and CdTe:AS; 2) CdTe:O_2 at 300 K.

photosensitivity spectra S_ω of Au- CdTe:O_2 diodes the sensitivity increases drastically for the energies exceeding the band gap of CdTe. It seems feasible to suggest that the observed quantum-scale surface texture is most probably formed by some kind of self-organization phenomena. This hypothesis is confirmed by a considerably narrow temperature and time intervals of the annealing process (Makhniy et al., 2003) that enable formation of the modified structure. Moreover, reproducing the same parameters under the different conditions (noble gas atmosphere or vacuum) does not lead to the desired effect, suggesting that one of the atmosphere components (in particular oxygen) plays an important role in the formation of a nano-crystalline surface structure. The definition of such dependence requires additional experimental and theoretical studies.

4. Electrical properties and carrier transport mechanisms

4.1 Potential barrier height

The height of the potential barrier φ_0 is one of the most important parameters of SBD: it limits open-circuit voltage U_{OC} of the photovoltaic device and enters the exponent in the expression describing over-barrier and tunneling currents, which with increase of φ_0 will yield a lower dark current. Also, higher barrier will favor a larger working temperature of a solar cell.

It was found out that the SBDs based on CdTe:AS and CdTe:O_2 feature significantly higher barrier than that achievable for the devices based on the non-modified CdTe. This point can be clearly seen from Fig. 6, where we plot forward-biased branches of current-voltage curves (CVCs) of the studied structures in their linearity region. It is important to highlight that the difference between the slopes of the segments for all three groups of diodes studied is insignificant, proving the close similarity of series resistance in the system diode base – deposited contacts. On the other hand, it also suggests that the contribution of the modified layer into the value of R_0 is negligibly small.

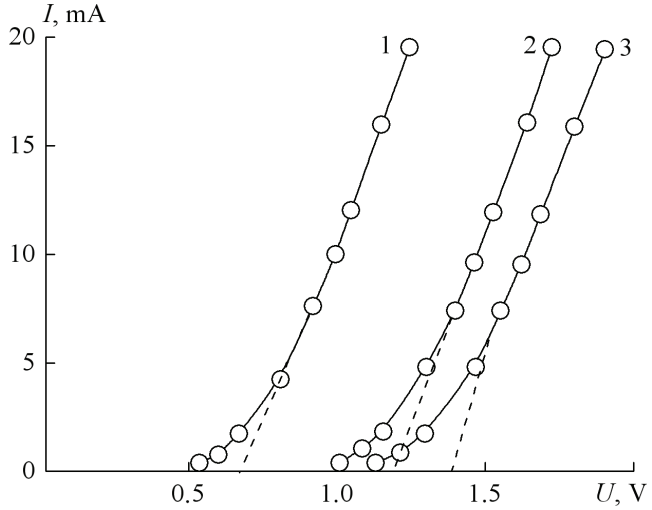

Fig. 6. Direct branches of CVC for the SBDs based on different substrates: 1) CdTe, 2) CdTe:AS, 3) CdTe:O_2 at 300 K.

The latter can be confirmed by the equal $I(U)$ dependence for the different diode types (Fig. 6). The same φ_0 and R_0 observable for the SBDs that differ by processing of their substrates (treatment in the solutions of Li, Na and K salts) suggest that various impurities have the same behavior in the resulting device. It is worth noting that the values of φ_0 determined from the direct CVC branches agree with the results obtained from the capacity measurements. The further analysis of the electrical properties revealed that the surface state apart from influencing φ_0 also change the character of physical processes in the SBDs, which is reflected in the dependences of forward / reverse currents as a function of voltage.

4.2 Direct current formation mechanisms in the surface barrier diodes

Figure 7 displays the initial segments of direct CVC branches measured for the modified surface diodes. As one can see from the figure, for $eU \geq 3kT$ the curves can be successfully approximated with the following expression (Rhoderick, 1978; Fahrenbruch & Bube, 1983)

$$I = I_0 \exp (eU / nkT) \tag{3}$$

where I_0 is a cut-off current at $U = 0$, and n is the non-ideality coefficient, which can be easily found as a slope of the straight CVC segments plotted in semi-logarithmic coordinates.
For Au-CdTe diodes the value of n is equal to the unity, suggesting the dominating over-barrier carrier transport for the SBDs made on the base of moderately-doped substrates (Rhoderick, 1978; Makhniy, 1992). It also means that the dielectric layer between metal and semiconductor is tunneling-transparent with the barrier height lower than $E_g/2$. The dependence $I_0(T)$ is mainly defined by the factor (Sze & Kwok, 2007)

$$I_0 \approx (- \varphi_0 / kT), \tag{4}$$

which gets an excellent confirmation in the experiment. Plotting $I_0(T)$ in $\ln I_0 - 1/T$ coordinates, one can achieve a good linear fit with the slope of 0.9 eV corresponding to φ_0 at 0 K.

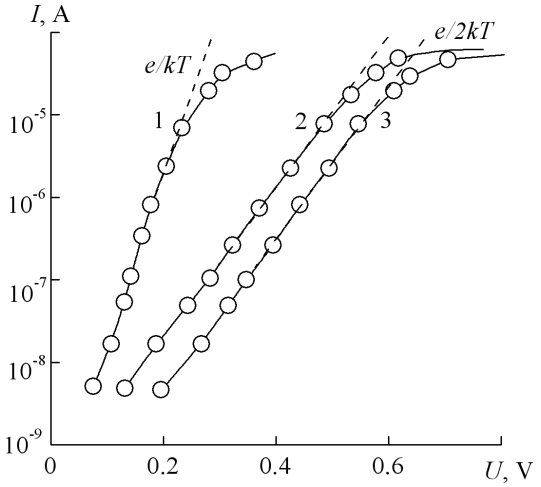

Fig. 7. The direct CVC branches of the diodes based on: 1) CdTe, 2) CdTe:AS and 3) CdTe:O_2 at 300 K.

In contrast to Au-CdTe contacts, the potential barrier height in the SBD with a modified surface will significantly exceed the value of E_g(CdTe)/2 = 0.75 eV at 300 K (Fig. 6). For such diodes the dominating carrier transport mechanism (Makhniy, 1992) is a recombination current in the space charge region (SCR) involving deep impurity levels. It can be also described by formula (3) with non-ideality coefficient n = 2. As one can see from Fig. 7, the initial direct CVC branches for Au-CdTe:AS and Au-CdTe:O_2 diodes fit excellently with the expression (3) for the temperature T = 300 K. However, it is also possible to approximate the experimental data with another exponential factor (Makhniy 1992)

$$I_0 \approx (-\varphi_0 / kT), \tag{5}$$

For this case, the measured $I_0(T)$ plotted in ln I_0 – $1/T$ coordinates will represent a straight line with a slope 1.6 eV corresponding to the band gap of cadmium telluride at 0 K.
Deviation of the experimental points from a straight line under the higher bias is caused by the voltage drop over series resistance of the diode, reducing the applied voltage U to the voltage at the barrier U_0 as

$$U_0 = U - IR. \tag{6}$$

Taking into account (6), one can re-write the expression (3) in the form (Makhniy 1992)

$$\ln I - \frac{eU}{kT} = \ln I_0 - \frac{eR_0}{nkT} I \,. \tag{7}$$

When the over-barrier current is dominating (which is correct for the voltages about φ_0) the non-ideality coefficient is equal to the unity and the direct branches of CVC can be efficiently plotted in the coordinates ln I_0 – eU/kT. These experimental data can be nicely fit with expression (7) in the case of the diodes with modified surface (Fig. 8) with ordinate interception yielding the ln I_0 for the given temperature.

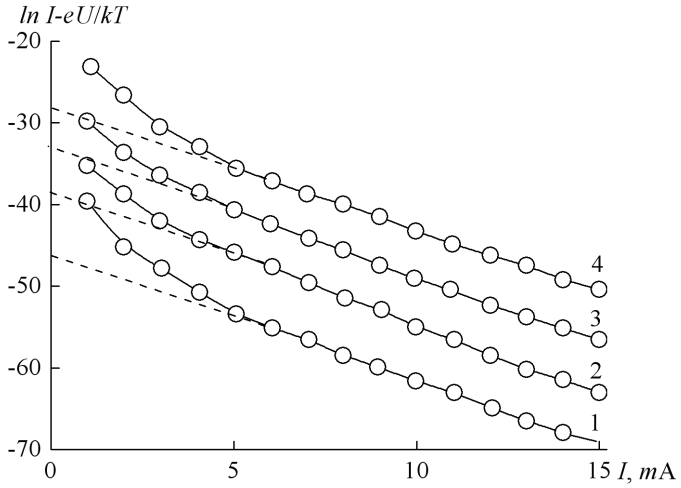

Fig. 8. Comparison of experimental data for direct CVC branches (Au-CdTe:AS diode) with theoretical formula (7) for the temperatures 1) 300 K, 2) 320 K, 3) 340 K and 4) 360 K

The dependence $I_0(T)$ obeys the expression (4) with φ_0 = 1.6 eV, which corresponds to the barrier height at 0 K. Taking into account the linear dependence $\varphi_0(T) = \varphi_0(0) - \gamma_\varphi T$ and using $\gamma_\varphi = 1.4 \cdot 10^{-3}$ eV/K one can estimate φ_0 = 1.18 eV at the room temperature, which correlates well with the experimental result 1.2 eV, Fig. 6.

While Fig. 8 presents the data for Au-CdTe:AS diode only, the similar results were obtained for all the structures studied. Therefore, the direct current transport in surface-barrier diodes based on CdTe has a predominant over-barrier character. In the diodes based on the substrates with a modified surface, the current is defined by carrier recombination in the space charge region (low direct bias) or over-barrier emission (high bias).

4.3 Reverse current in surface barrier diodes

It is important to emphasize that over-barrier and recombination cut-off currents I_0 at 300 K are always below 10^{-10} A (Fig. 7). Moreover, these currents in a theoretical model feature a weak dependence on the voltage, such as $U^{1/2}$ (Rhoderick, 1978; Sze & Kwok, 2007). However, in the experiments we obtained steeper curve of inverse current I_{inv}(U), suggesting other current transport mechanisms.

It is logical to assume that in the SBDs based on wide-band semiconductors (which holds for CdTe) subjected to inverse bias tunneling of the carriers will become a dominating mechanism, including both inter-band tunneling and tunneling *via* the local levels (Makhniy, 1992). The validity of this hypothesis is supported by Fig. 9, where the inverse CVC exhibit a good fitting with the formula for tunneling current in an abrupt junction:

$$I_{inv} = a \exp\left(-\frac{b}{\sqrt{\varphi_0 - eU}} \right). \tag{8}$$

Here a and b are the coefficients that can be found from the parameter substrate and the diode structure. The negative sign under the square root reflects the negative bias, and the voltage in the expression (8) should be substituted with the negative sign. The high slope of

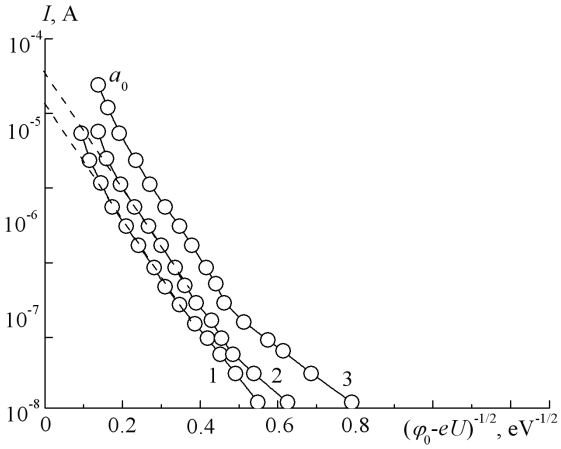

Fig. 9. Comparison of theoretical calculations according to (8) with the inverse CVC branches for the diodes based on: 1) CdTe, 2) CdTe:AS, and 3) CdTe:O_2 at 300 K.

the initial branches of inverse CVCs signals the parameter difference for the diode structures but not the substrates themselves. It is worth noting that the coefficient b depends on the height and width of the barrier, the depth of the local centers in the SCR and some other parameters (Makhniy, 1992), which requires more detailed study. The same can be commented concerning the dependence $I_{inv}(U)$ under high bias (Fig. 9), which in addition to tunneling may have also include the avalanche processes (Mizetskaya et al., 1986).
While the solution of the aforementioned tasks is important for the photodiodes, it is not that much crucial for solar cell applications that require a special attention to the parameters φ_0, n, I_0, and E_g appearing in the expression for the direct current.

5. Photoelectric properties of surface barrier diodes

5.1 Integral illuminated current voltage curves

The CVC of illuminated diode can be described as (Fahrenbruch & Bube, 1983; Koltun, 1987)

$$I = I_0\left[\exp\left(\frac{eU}{nkT}\right)-1\right]-I_p \tag{9}$$

with photocurrent I_p, dark current $I_0(U = 0)$ and non-ideality coefficient n, which is determined by the current transport mechanism. To determine the exact mechanisms involved in formation of CVCs for illuminated solar cells, we need introduce open circuit voltage (at $I = 0$) and short circuit current I_{SC} (for $U = 0$) that upon being substituted into (9) for a particular case $eU \geq 3kT$ would yield the expression

$$I_p = I_{SC} = I_{SC}^0 \exp\left(eU_L / nkT\right). \tag{10}$$

Here I_{SC}^0 denotes the cut-off current for illuminated cell voltage $U_L = 0$, which may coincide with I_0 only in the case if the formation mechanisms for the light and dark currents are the same. Therefore, investigation of the integral light CVCs allow to determine the corresponding current formation mechanism, as well as to reveal both common and

different traits between the electric and photoelectric properties of the materials studied. Analysis of $I_{SC}(U_{OC})$ curves shows that they are qualitatively similar, differing only in non-ideality value for the various SBD groups. Thus, for Au-CdTe diodes the value of n = 1 suggests over-barrier transport of photo-generated carriers, which can be also illustrated by fitting data presented in Fig. 10 (curve 1). It is worth mentioning that I_{SC}^{0} is close to the cut-off current I_0, obtained for the dark CVC for the same diode at 300 K.

The energy slope of the segment $\ln I_{SC}^{0} - 1/T$ yields the value of 0.9 eV that coincide with the potential barrier height φ_0 at 0 K, determined from the temperature dependence of the dark cut-off current I_0. In this way, one can conclude that dark and light currents of Au-CdTe contacts are formed by over-barrier emission of the carriers. To the contrary, the measured CVC of the illuminated SBDs with a modified surface will require non-ideality coefficient to be n=2, equation (10), to achieve the appropriate fitting illustrated in Fig. 10 (curve 2) for Au-CdTe:AS diode. As it was mentioned before, such dependence is characteristic for carrier recombination in the space charge region involving local centers, while the photosensitivity data for Au-CdTe suggests the dominating inter-band generation of the carriers.

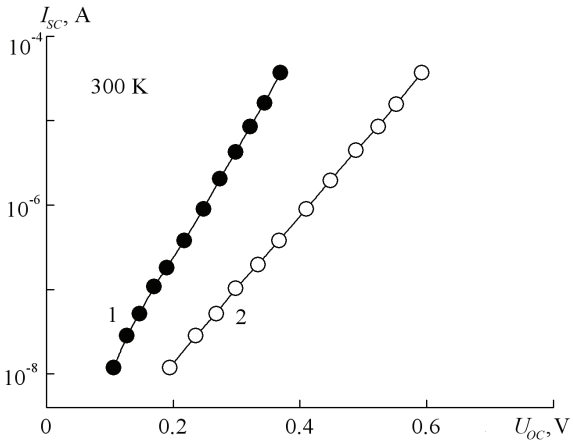

Fig. 10. Dependence of short circuit current on the open circuit voltage for Au-CdTe (1) and Au-CdTe:AS (2) diodes.

This controversy can be eliminated (Ryzhikov, 1989): under the stationary conditions the carrier generation rate G should be equal to the recombination rate R. However, if these phenomena are caused by distinct mechanisms, they will be described by the different analytical expressions. It is worth mentioning that the measurement of the dependences $I_{SC}(U_{OC})$ is performed in so-called compensation mode, when the photocurrent is equalized with dark current under the presence of direct bias. Due to this, one actually monitors recombination of photo-carriers, which yields the expression similar to that of the dark current. It is important that for the SBDs based on the substrates with a modified surface the dark current under the low direct bias is controlled by the recombination processes in space charge region (see Section 4). As carrier generation in the surface barrier diodes takes place in the space charge region due to the fundamental absorption of high-energy photons with $\hbar\omega > E_g$, it is more probable that they will recombine at the same device region taking advantage of the local impurity centers rather than *via* the inter-band recombination.

5.2 Dependence of I_{SC} and U_{OC} on illumination level and the temperature

For all the SBDs studied, the short circuit current depends linearly on the power of the incident light flux L, which is a consequence of linearity of photo-carrier generation as

$$I_{SC} = \beta L, \tag{11}$$

where β is a proportionality coefficient independent on L. As one can see from Fig. 11, the equation (11) holds well for illumination power spanning over several orders of magnitude. Using the expressions (10) and (11) it is easy to show that

$$U_{OC} = nkT\left(\ln\left(I_{SC} / I_{SC}^{0}\right)\right) = nkT\ln\left(\beta L / I_{SC}^{0}\right). \tag{12}$$

As one can see from Fig. 12, expression (12) describes well the experimental dependences of $U_{OC}(L)$ for the low illumination conditions. The tendency of $U_{OC}(L)$ curves to saturate under high L is caused by the potential barrier compensation. The higher value of U_{OC} for the SBDs with a modified surface in comparison with that of Au-CdTe diodes is explained by the significant difference of potential barrier heights for these rectifying structures (see Sec. 2).

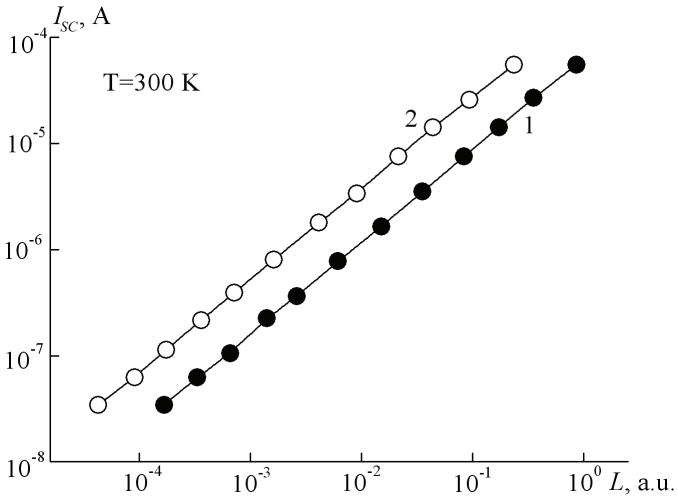

Fig. 11. Dependence of short circuit current on radiation power for Au-CdTe (1) and Au-CdTe:AS (2) diodes

Our investigations revealed that the temperature increase leads to a slight growth of short circuit current, which is caused by an insignificant decrease of series resistance R_0 characterizing the device. Under high illumination open circuit voltage tends to saturate, so that in the first approximation $U_{OC} \approx \varphi_0$ or E_g depending on formation mechanism of the light CVCs (see above). Therefore, under otherwise equal conditions, the open circuit voltage should diminish with increase of temperature, which was confirmed experimentally for all SBDs studied. It is important to emphasize that $U_{OC}(T)$ curve for SBDs with a modified surface features much weaker slope than that observable for the reference diodes. This can be explained by the different temperature dependence of variation coefficient for the band gap E_g and barrier height γ_φ (see Sec. 4).

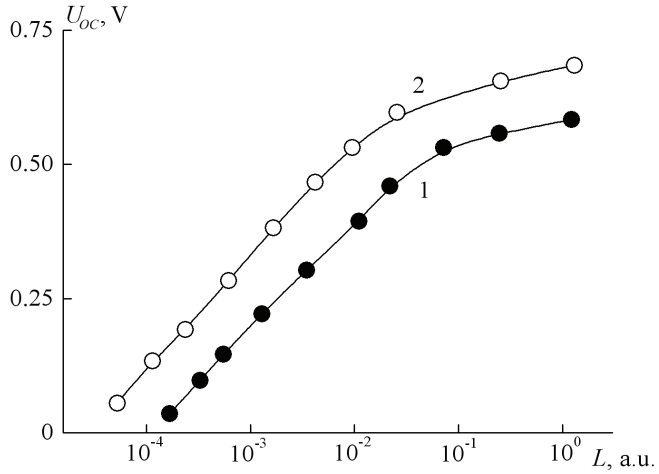

Fig. 12. Dependence of open circuit voltage on the illumination level for Au-CdTe (1) and Au-CdTe:AS (2) diodes

5.3 Spectral characteristics

The previous investigations of optical, electrical and photoelectrical properties of the SBDs predict several peculiar and promising characteristics of these structures. In the first place, the low energy limit $\hbar\omega_{min}$ of the photosensitivity spectrum S_ω is determined with high-energy edge of the transmission spectrum. According to the data presented in Fig. 5, the low-energy edge of S_ω curves for Au-CdTe and Au-CdTe:AS diodes will be about 1.5 eV, while for Au-CdTe:O_2 contacts it is somewhat lower, reaching 1.3 eV (Fig. 13).

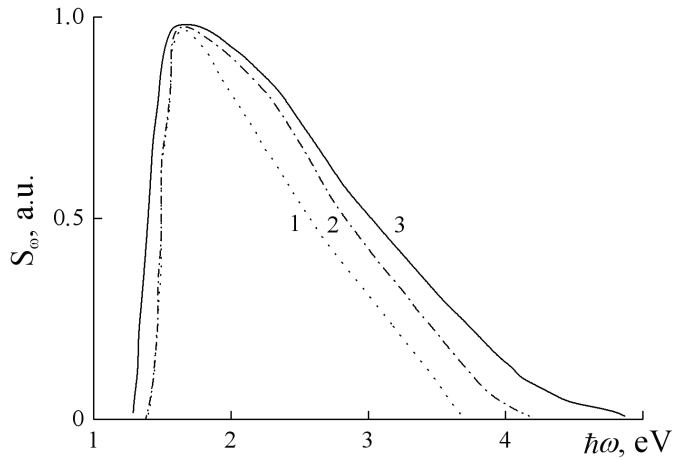

Fig. 13. Photosensitivity spectra for the SBD based on the substrates of CdTe (1), CdTe:AS (2) and CdTe:O_2 (3) at 300 K

High-energy photosensitivity, as it was discussed above, is defined by the surface recombination rate, which in turn depends on concentration of the defects N_S at the junction

boundary. Thus, high short-wave sensitivity should be expected in SBDs based on the substrates with a maximum efficiency of edge luminescence band. This conclusion is confirmed by the data presented in Fig. 13, featuring wider photo-sensitivity peaks for Au-CdTe:O_2 diodes, which are based on the substrates with the most intensive A-band (see Section 3) reaching 10% for 300 K. At the same time, for case of CdTe:AS and CdTe substrates, the corresponding A-band values would be 1-2% and 0.01%, respectively, strongly influencing the behavior of S_ω spectra for photon energies $\hbar\omega > E_g$ (Fig. 13).
Investigation of the temperature dependence of the SBD spectra reveals that higher values of T mainly affect their low-energy "tail". The edge of S_ω under the temperature varying in the ranges 300-450 K almost replicates the dependence $E_g(T)$. In the contrast to this, the temperature dependence of the surface defects (*i.e.*, their concentration, energy distribution and scattering cross-sections) is negligibly weak, as one may conclude from the photosensitivity spectra for $\hbar\omega > E_g$.

Type of the surface barrier diode		Au-CdTe	Au-CdTe:AS	Au-CdTe:O_2
Parameters	φ_0, eV	0.7	1.2	1.35
	R_0, Ω	30	30	32
	U_{OC}, V	0.4	0.6	0.7
	I_{SC}, mA/cm²	10	15	22
	Efficiency, %	5	9	13

Table 1. Main parameters of the solar cells

5.4 Main parameters of surface barrier solar cells

The diodes with the effective photosensitive area of $2 \cdot 10^{-2}$ cm² were illuminated from the side of a semi-transparent golden contact by light equivalent to AM2 solar illumination conditions. All the measurements were performed at 300 K and the best results obtained were summarized in Table 1.
The values characterize photovoltaic devices in "as-obtained" form without anti-reflection coatings or any special optimization of solar cell design. Due to this, the values of fill factor *ff* are under 0.7 because of considerable series resistance (see Table 1). The reduction of the latter would allow increase of both I_{SC} and *ff*, improving the efficiency of the SCs.

6. Conclusions

The authors developed a special technological approach consisting in a special surface treatment of monocrystalline plates of cadmium telluride before deposition of the barrier contact, which significantly improves the electrical and photoelectric properties of the surface-barrier devices of metal-semiconductor junction type created on their base. The

annealing of n-CdTe substrates (ρ ~ 10-20 Ω cm) in the air or aquatic suspense of alkaline metals increases the potential barrier height φ_0 up to 1.2-1.4 eV in comparison with $\varphi_0 \approx 0.7$ eV for non-annealed substrates. The SBDs with modified surface features much better open circuit voltage and short circuit current. The efficiency of solar cells based on the diodes studied under AM2 illumination was within the ranges 8-13% at the room temperature. The developed technology for surface-barrier solar cells is simple, cheap and ecologically clean. In addition, the proposed technological principles can be used for producing photovoltaic devices based on thin films of cadmium telluride.

7. Acknowledgements

This research was supported in part by the Ministry for Education and Science (Ukraine) through the financing provided for the scientific projects carried out at the Department of Optoelectronics, Department of Energy Engineering and Electronics, as well as at the Science and Education Center "Semiconductor Material Science and Energy-Efficient Technology" at the Chernivtsi National University, Research Project #SU/447-2009 for the years 2009-2010. We also acknowledge the financial support of CONACYT (México) for the research performed in CINVESTAV-Querétaro, Research Project CB-2005-01-48792 for the years 2007-2010.

8. References

Alferov, Zh.I. (1998). The history and the future of semiconductor structures. *Fiz. Tekhn. Poluprov.*, Vol. 32, No. 1, 3-19

Amanullah, F.M. (2003). Effect of isochronal annealing on CdTe and the study of electrical properties of Au–CdTe Schottky devices. *Canadian Journal of Physics*, Vol. 81, No. 3, 617-624

Andreev, V.M.; Dolginov, L.M. & Tret'yakov. D.N. (1975). *Liquid epitaxy in technology of semiconductor devices*, Soviet radio, Moscow

Batavin, V.V.; Kontsevoj, Yu.A. & Fedorovich. Yu.V. (1985). *Measurement of the parameters of semiconductor materials and structures*, Radio i svyaz', Moscow

Britt, J. & Ferekides, C. (1993). Thin film CdS/CdTe solar cell with 15.8% efficiency. *Applied Physics Letters*, Vol. 62, 2851-2852

Chopra, K.L. & Das, S.R. (1983). *Thin film solar cells*, Springer, New York

Ciach, R.; Demich, M.V.; Gorley, P.M.; Kuznicki, Z.; Makhniy, V.P.; Malimon, I.V. & Swiatek, Z. (1999). Photo and X-ray sensitive heterostructures based on cadmium telluride, *J. Cryst. Growth*, Vol. 197, No. 3, 675-679

Donnet, D. (2001). Cadmium telluride solar sells. In: *Crean Electricity from Photovoltaic*. Archer, M.D. & Hill, R. (Eds.), 245-276, Imperial College Press

Fahrenbruch, A.L. & Bube, R.H. (1983). *Fundamentals of solar cells: photovoltaic solar energy conversion*. Academic Press, New York

Gnatyuk, V.A.; Aoki, T.; Hatanaka, Y. & Vlasenko, O.I. (2005). Metal–semiconductor interfaces in CdTe crystals and modification of their properties by laser pulses, *Applied Surface Science*, Vol. 244, 528-532

Higa, A.; Owan, I.; Toyama, H.; Yamazato, M.; Ohno, R. & Toguchi, M. (2007). Properties of Al Schottky Contacts on CdTe(111)Cd Surface Treated by He and H_2 Plasmas *Japanese Journal of Applied Physics*, Vol. 46, 2869-2872

Kesamanly, F.P. & Nasledov, D.N. (Eds.) (1973). *Gallium arsenide: production, properties and applications*, Nauka, Moscow

Kim, K.; Cho, S.; Suh, J. Won, J. Hong, J. & Kim. S. (2009). Schottky-type polycrystalline CdZnTe X-ray detectors. *Current Applied Physics*, Vol. 9, No. 2, 306-310

Koltun, M.M. (1985). *Optics and metrology of the solar cells*, Nauka, Moscow

Koltun, M.M. (1987). *Solar cells*, Nauka, Moscow

Korbutyak, D.V.; Mel'nychuk, S.V.; Korbut, Ye.V. & Borysyuk, M.M. (2000). *Cadmium telluride: impurity defect states and detector properties*, Ivan Fedoriv, Kyiv

Madelung, O. (2004). *Semiconductors: Data Handbook*, Springer

Makhniy, V.P. & Skrypnyk, M.V. (2008). Patent for the useful model UA №31891 published 25.04.2008.

Makhniy, V.P. (1992). *Physical processes in the diode structures based on wide-band A^2B^6 semiconductors*. Dissertation of the Doctor in Physics and Mathematics, Chernivtsi

Makhniy, V.P.; Demych, M.V. & Slyotov, M.M. (2003). Declaration patent UA №5010A published 22.04.2003.

Makhniy, V.P.; Skrypnyk, M.V. & Demych, M.V. (2009a). Patent for a useful model UA №40056 published 23.05.2009.

Makhniy, V.P.; Slyotov, M.M. & Skrypnyk, N.V. (2009b). Peculiar optical properties of modified surface of monocrystalline cadmium telluride, *Ukr. J. Phys. Opt.*, Vol. 10, No. 1, 54-60

Makhniy, V.P.; Slyotov, M.M.; Stets, E.V.; Tkachenko, I.V.; Gorley, V.V. & Horley, P.P. (2004). Application of modulation spectroscopy for determination of recombination center parameters. *Thin Solid Films*, Vol. 450, 222-225

Mason, W.; Almeida, L.A.; Kaleczyc, A.W. & Dinan, J.H. (2004). Electrical characterization of Cd/CdTe Schottky barrier diodes. *Applied Physics Letters*, Vol. 85, No. 10, 1730-1732

Milnes, A. & Feucht, D. (1972). *Heterojucntions and metal semiconductor junctions*, Academic Press, New York

Mizetskaya, I.B.; Oleynik, G.S.; Budennaya, L.D.; Tomashek, V.N. & Olejnik. N.D. (1986). *Physico-chemical bases for the synthesis of monocrystals of semiconductor solid solutions $A^{II}B^{VI}$*, Naukova dumka, Kiev

Pool, Ch. Jr. & Owens, F. (2006). *Nanotechnologies*, Tekhnosfera, Moscow

Rhoderick, E.H. (1982). *Metal-semiconductor contacts*, Clarendon Press, Oxford

Ryzhikov, V.D. (1989). *Scintillating crystals of the semiconductor compounds A^2B^6: Obtaining, properties, applications*, NIITEKhIM, Moscow

Sharma, B.L. & Purohit, R.K. (1979). *Semiconductor heterojunctions*, Soviet radio, Moscow

Simashkevich, A.V. (1980). *Heterojunctions based on semiconductor $A^{II}B^{VI}$ compounds*, Sthtiintsa, Kishinev

Sites, J. & Pan, J. (2007). Strategies to increase CdTe solar-cell voltage. *Thin Solid Films*, Vol. 515, No. 15, 6099-6102.

Strikha, V.I. & Kil'chitskaya, S.S. (1992). *Solar cells based on the contact metal-semiconductor*, Energoatomizdat, St. Petersburg

Sze, S.M. & Kwok, K.Ng. (2007). *Physics of semiconductor devices*, J. Willey & Sons, New Jersey
Valiev, K.A.; Pashintsev, Yu.I. & Petrov, G.V. (1981). *Using contacts metal-semiconductor in electronics*, Soviet radio, Moscow
Vorobiev, Yu.V.; Dobrovol'skiy, V.N. & Strikha, V.I. (1988). *Methods in semiconductor studies*, Vyshcha shkola, Kiev
Zayachuk, D.M. (2006). *Low-scale structures and super-lattices*, Lviv Polytechnic, Lviv

Solar Energy

Edited by Radu D Rugescu

ISBN 978-953-307-052-0
Hard cover, 432 pages
Publisher InTech
Published online 01, February, 2010
Published in print edition February, 2010

The present “Solar Energy” science book hopefully opens a series of other first-hand texts in new technologies with practical impact and subsequent interest. They might include the ecological combustion of fossil fuels, space technology in the benefit of local and remote communities, new trends in the development of secure Internet Communications on an interplanetary scale, new breakthroughs in the propulsion technology and others. The editors will be pleased to see that the present book is open to debate and they will wait for the readers’ reaction with great interest. Critics and proposals will be equally welcomed.

How to reference

In order to correctly reference this scholarly work, feel free to copy and paste the following:

P.M. Gorley, V.P. Makhniy, P.P. Horley, Yu.V. Vorobiev and J. González-Hernández (2010). Surface-Barrier Solar Cells Based On Monocrystalline Cadmium Telluride with the Modified Boundary, Solar Energy, Radu D Rugescu (Ed.), ISBN: 978-953-307-052-0, InTech, Available from: http://www.intechopen.com/books/solar-energy/surface-barrier-solar-cells-based-on-monocrystalline-cadmium-telluride-with-the-modified-boundary

INTECH
open science | open minds

InTech Europe
University Campus STeP Ri
Slavka Krautzeka 83/A
51000 Rijeka, Croatia
Phone: +385 (51) 770 447
Fax: +385 (51) 686 166
www.intechopen.com

InTech China
Unit 405, Office Block, Hotel Equatorial Shanghai
No.65, Yan An Road (West), Shanghai, 200040, China
中国上海市延安西路65号上海国际贵都大饭店办公楼405单元
Phone: +86-21-62489820
Fax: +86-21-62489821